Expanded View Figures

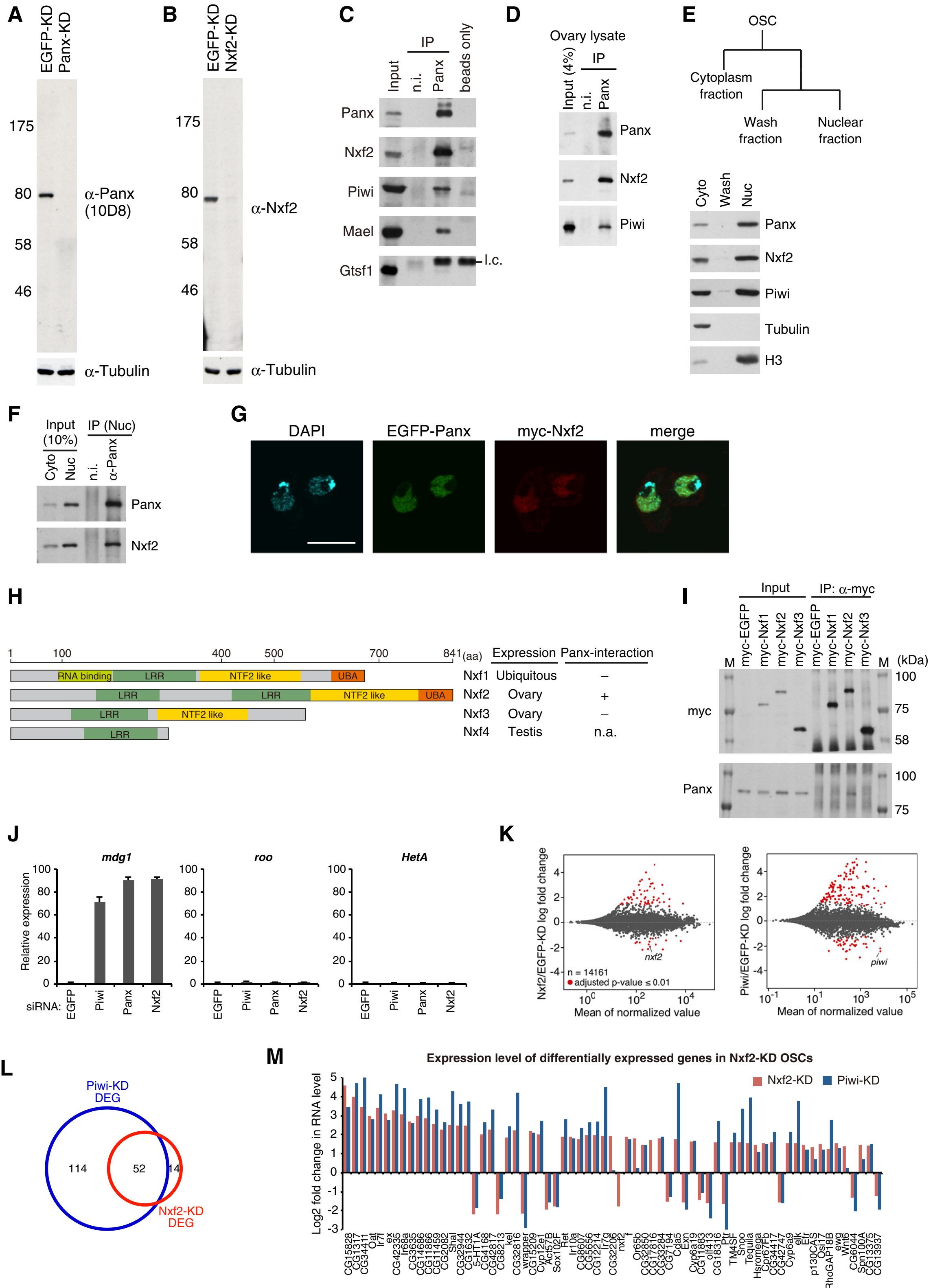

Figure EV1.

◀ **Figure EV1. Nxf2 associates with Panx and Piwi to regulate piRNA target TEs.**

A Western blotting (WB) shows the specificity of anti-Panx monoclonal antibodies raised in this study. Tubulin was used as a loading control.

B WB shows the specificity of anti-Nxf2 monoclonal antibodies raised in this study.

C Immunoprecipitation (IP) from OSC lysate using anti-Panx antibody, followed by WB of Panx, Nxf2, Piwi, Mael, and Gtsf1. IP-WB was performed under the same conditions as the silver staining described in Fig 1A. Mouse immunoglobulin G (IgG) (n.i.) was used for control IP. l.c.: light chain from the antibody.

D IP from fly ovary lysate using anti-Panx antibody, followed by WB of Panx, Nxf2, and Piwi.

E Scheme of preparation of cytoplasmic and nuclear fractions of OSCs. WB using Panx, Nxf2, Piwi, Tubulin, and histone H3 antibodies shows the level of each protein in the separate fractions. Tubulin was detected in the cytoplasmic fraction, where histone H3 was enriched in the nuclear fraction.

F IP from nuclear OSC lysate using anti-Panx antibody, followed by WB.

G Immunofluorescence of OSCs co-transfected with EGFP-Panx- and myc-Nxf2-expressing vectors, using myc antibody (red). EGFP is detected as Panx signal, and DAPI staining (blue) shows the location of nuclei. EGFP-Panx and myc-Nxf2 co-localize in the nucleus. Scale bar: 10 μm.

H Schematic of NXF variants. LRR: leucine-rich repeat, NTF2-like: nuclear transport factor 2-like domain, UBA: ubiquitin-associated domain (left panel). Nxf1 is ubiquitously expressed, while Nxf2 and Nxf3 are almost exclusively expressed in ovary, and Nxf4 is specifically expressed in testis. The interaction between Nxf4 and Panx was not analyzed, since Nxf4 expression is limited to testis, indicated as n.a. (not available) (right panel).

I IP from lysate of OSCs expressing myc-tagged NXF variants, followed by WB using anti-myc and anti-Panx antibodies. M indicates protein markers. The results are summarized in the right panel in (H). Among NXF variants, only Nxf2 can interact with Panx.

J RNA levels of *mdg1*, *roo*, and *HetA* were quantified by qRT–PCR upon depletion of EGFP (control), Piwi, Panx, or Nxf2. Expression levels are normalized by the expression of *RP49*. Error bars represent SD ($n = 3$). Piwi–piRNA-targeted TE was specifically de-silenced by Piwi-, Panx-, and Nxf2-KD, confirming the results of RNA-seq.

K MA plot of RPKM values ($\log_{10}$ scale) for mRNAs in the indicated KD samples, based on RNA-seq. Differentially expressed genes (DEGs) are in red.

L Venn diagram displaying the number of DEGs upon depletion of Nxf2 (red) or Piwi (blue).

M Log_2 fold changes in mRNA levels of 67 DEGs in Nxf2-KD OSCs. mRNA levels calculated from RNA-seq data are used for Nxf2- and Piwi-KD OSCs. Most mRNAs whose expression was altered upon Nxf2-KD were also affected by Piwi-KD, suggesting that Nxf2 does not globally affect mRNA levels.

© 2019 The Authors

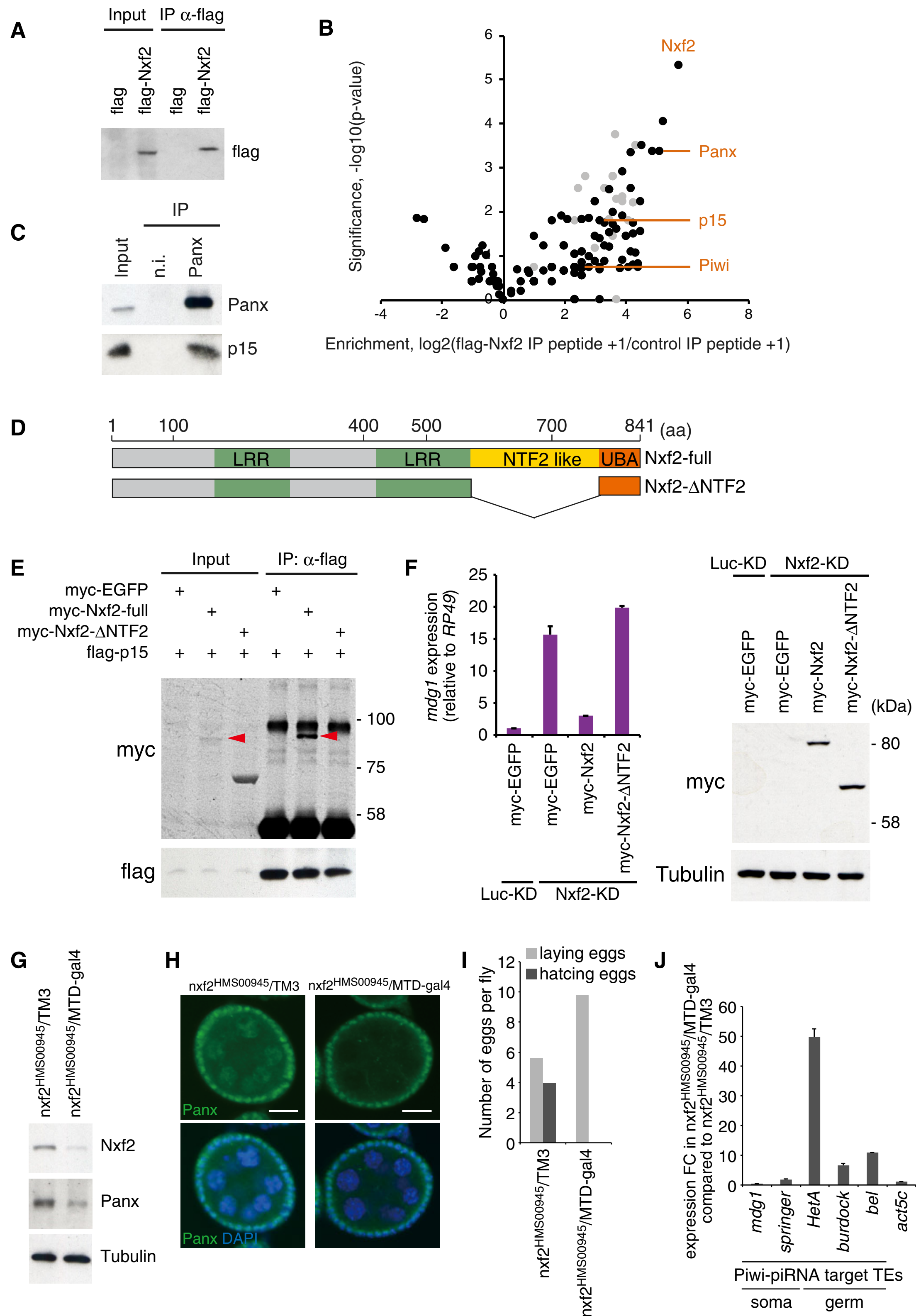

Figure EV2.

Figure EV2. p15 interacts with Nxf2 at its NTF2-like domain.

A Western blot (WB) showing flag–Nxf2 immunoprecipitant from OSCs expressing either flag only (control) or flag–Nxf2, using flag antibody. The immunoprecipitant was subjected to proteome analysis.
B Summary of the proteome analysis of peptide-eluted flag–Nxf2 component. The plot shows the enrichment of peptide obtained by flag-Nxf2 immunoprecipitation (IP) over control IP ($\log_2$ value of peptide count + 1) on the *x*-axis, and significance calculated by replicate experiments as the Student's *t*-test *P*-value ($-\log_{10}$) on the *y*-axis. Enrichment and significance of each protein are listed in Appendix Table S2. Ribosomal proteins are plotted in gray.
C IP from OSC lysate using anti-Panx antibody, followed by WB of Panx and p15. IP was performed under the same conditions as silver staining described in Fig 1A.
D Schematic of full-length Nxf2 protein and deletion mutant of NTF2-like domain (Nxf2-ΔNTF2).
E Flag-IP performed using lysate of flag-p15- and myc-EGFP- or myc-Nxf2-ΔNTF2-expressing OSCs, followed by WB using myc or flag antibody. myc-Nxf2-full is indicated by a red arrowhead. p15 cannot interact with the Nxf2 construct lacking NTF2-like domain.
F myc-EGFP, myc-Nxf2, and myc-Nxf2-ΔNTF2 were expressed in Luc- (control) or Nxf2-depleted OSCs. *mdg1* expression levels were monitored by qRT–PCR. Expression values are normalized by the expression of *RP49*. Error bars indicate SD (n = 3) (left panel). WB using an antibody against myc and tubulin using lysates from transfected OSCs (right). The ΔNTF2 deletion mutant, which cannot interact with p15, could not rescue the silencing of TE.
G WB of ovaries from nxf2HMS00945/MTD-gal4 flies using Nxf2, Panx, and tubulin (control) antibody. Note that the expression of shRNA is limited to germline cells by MTD-gal4. Depletion of Nxf2 in the germline cells also results in a decrease of Panx protein level.
H Immunofluorescence of ovaries from nxf2HMS00945 flies using Panx antibody (green). DAPI staining (blue) shows the location of nuclei. Decrease of Panx in Nxf2-depleted ovaries was observed specifically in the germ cells. Scale bars: 20 μm.
I Numbers of eggs laid and hatched per fly are indicated. Nxf2 depletion in *Drosophila* ovaries results in sterility phenotype.
J mRNA levels of Piwi–piRNA-targeted TEs and *actin 5c* (control) were quantified by qRT–PCR. Expression values are normalized by the expression of *RP49*. Error bars represent SD (n = 3). Piwi–piRNA-targeted TEs in the germ cells were specifically de-silenced upon germline-specific Nxf2 depletion.

 © 2019 The Authors

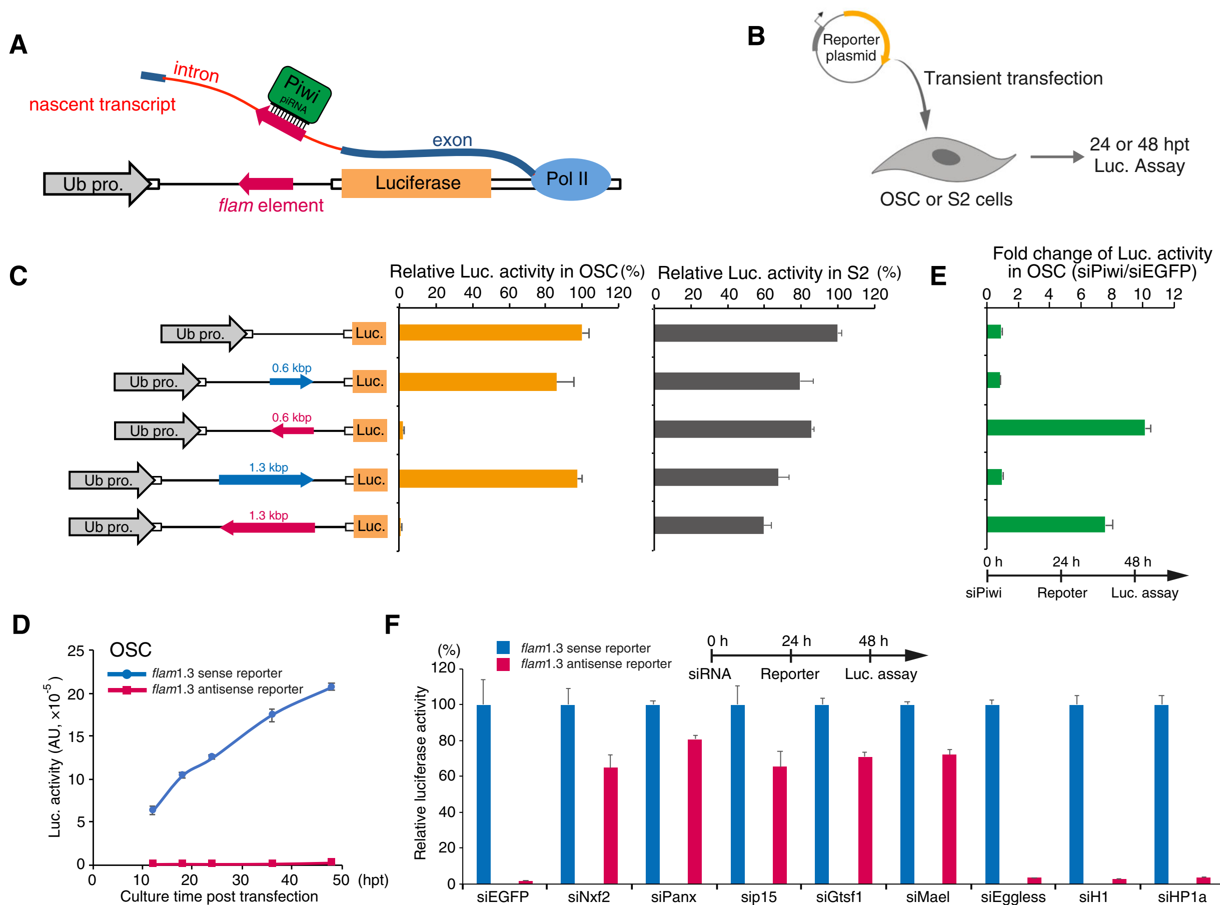

Figure EV3. The PPNP complex is required for the co-transcriptional silencing in the Piwi-piRNA-targeted reporter system.

A Schematic of piRNA reporter gene assay. Reporter plasmid carries *flam* element in its intron. *Luc* mRNA harboring *flam* element in the antisense direction is targeted by Piwi carrying piRNAs derived from the *flam* locus.

B Experimental scheme. OSCs or S2 cells were transfected with reporter plasmids transiently and harvested at 24 or 48 hpt.

C Left panel shows reporter gene constructs harboring *flam* elements (0.6 kbp or 1.3 kbp) inserted in the intron. Blue and red arrows indicate sense and antisense directions, respectively. Middle graph shows luciferase activity relative to that of reporter gene without *flam* elements in OSC. Right graph shows luciferase activity relative to that of reporter gene without *flam* elements in S2 cells. Error bar indicates SD ($n = 4$). The sense reporters were expressed similar to control reporter gene lacking the *flam* element, whereas the antisense (piRNA-targeted) reporters were completely silenced, even though we introduced the reporter gene as a plasmid into OSCs, suggesting that the co-transcriptional silencing occurs independent of the chromatin context.

D Time course of luciferase activity in OSCs. Blue and red arrows indicate reporter gene bearing a flam element (1.3 kbp) in the sense or antisense direction, respectively. Error bar indicates SD ($n = 3$).

E Silencing of reporter gene harboring *flam* element (1.3 kbp, antisense direction) occurs in a Piwi-dependent manner. Graph shows fold change of luciferase activity in OSCs treated with siPiwi or siEGFP (control). Error bar indicates SD ($n = 3$).

F Effects of knockdown of the indicated genes on piRNA reporter activity (1.3 kbp, *flam*). Red bar shows the luciferase activities of the antisense reporter relative to that of the sense reporter (blue). Error bars indicate SD ($n = 3$). Transfection schedule of siRNA and reporter plasmids is shown at the top of the figure. Depletion of Nxf2, Panx, p15, and known cofactors Gtsf1 and Mael, de-silenced the piRNA-targeted reporter in OSCs. In contrast, Eggless-KD, H1-KD, and HP1-KD had no impact on the silencing.

© 2019 The Authors

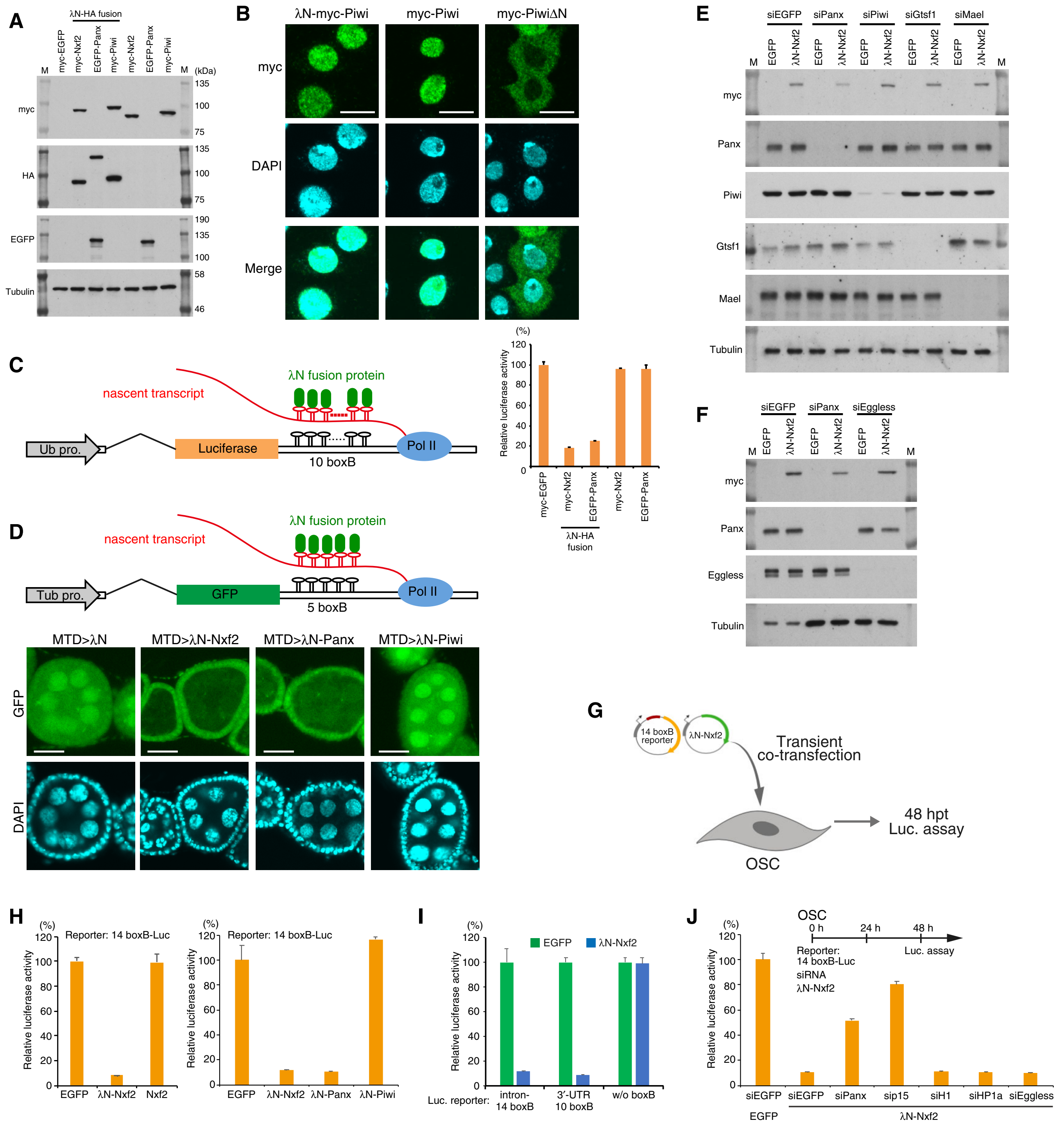

Figure EV4.

 © 2019 The Authors

Figure EV4. Enforced tethering of Nxf2 to nascent mRNA causes co-transcriptional silencing.

A Western blotting (WB) associated with Fig 3B shows the exogenous expression of λN-fused proteins. Nxf2 and Piwi were tagged with λN-HA and myc, whereas Panx was tagged with λN-HA and EGFP, since the expression level of EGFP–Panx was higher than the level of myc-tagged Panx, which is quite unstable. M indicates protein markers.

B Immunofluorescence of OSCs transfected with λN-myc-Piwi-, myc-Piwi-, or myc-PiwiΔN-expressing vectors, using myc antibody (Green). DAPI staining (blue) shows the location of nuclei. myc-PiwiΔN lacking nuclear localization signal (NLS) was distributed in cytoplasm (Saito *et al*, 2010; Yashiro *et al*, 2018). λN-myc-Piwi localized in the nucleus similarly to myc-Piwi, indicating that λN-myc-Piwi harbored piRNA in OSCs, even though it failed to induce silencing of the boxB reporter gene (Fig 3B, see also Fig EV4D and H). This may be due to only Piwi, which is guided to the target via its loaded piRNAs, potentially being able to recruit silencing machinery to the target (see also Fig EV3C and Appendix Fig S2I). Scale bars: 10 μm.

C Schematic of boxB-λN tethering system in OSCs shows a genome-integrated luciferase reporter with 10 copies of boxB sites located within the 3′ UTR of *luc* mRNA (left). Bar graph shows relative luciferase activity normalized by total protein amount at 48 h post-transcription (right). Error bars indicate SD (n = 4). Tethering of Nxf2 and Panx to the 3′ UTR of *luc* mRNA leads to silencing in OSCs.

D Schematic of boxB-λN tethering system in fly ovary shows a genome-integrated *GFP* reporter with five copies of boxB sites located within the 3′ UTR of *GFP* mRNA. λN-fused proteins are driven by MTD-Gal4. Tub pro: *α-Tubulin* gene promoter (top panel). Confocal images depict GFP fluorescence and DAPI signals in egg chambers expressing the indicated λN fusion proteins in the germline. Expression of λN-Nxf2 and Panx leads to reporter silencing in germ cells, but that of λN-Piwi does not. This is consistent with our data in Fig 3B and previous reports (Sienski *et al*, 2015; Yu *et al*, 2015). Scale bars: 20 μm.

E, F Results of WB associated with Fig 3E and 3F, showing the expression of λN-HA–myc-Nxf2 and the effect of siRNAs on target gene expression.

G Experimental design. According to Fig EV3B, the reporter genes do not have to be integrated into the genome, suggesting that the co-transcriptional silencing occurs independent of the chromatin context. To examine this issue, we carried out co-transfection of reporter plasmid (14 boxB-Luc) and expression plasmids for λN fusion protein to OSCs, transiently. Cells were harvested at 48 hpt.

H Effect on luciferase activity of the proteins indicated below. Error bars indicate SD (n = 4). Even if a plasmid with 14 boxB reporter sites was transiently introduced into OSCs, λN-Nxf2 repressed luciferase activity.

I λN-Nxf2 represses luciferase activity of reporter plasmid harboring 10 boxB sites in its 3′ UTR, but not that of reporter plasmid without boxB. Error bars indicate SD (n = 4).

J Effects of knockdown of the indicated genes on boxB reporter activity upon λN-Nxf2 expression. Bar graph shows luciferase activity relative to that of the sample co-transfected with myc-EGFP and siEGFP (control). Error bars indicate SD (n = 4). Transfection schedule of siRNA and reporter plasmids is shown at the top of the figure. Although knockdown of Panx and p15 weakened the repression by the forced tethering of Nxf2, the effects of H1- and HP1a-KD on the λN-Nxf2-mediated silencing were negligible, which is consistent with the results from Figs 4D and EV3F.

© 2019 The Authors

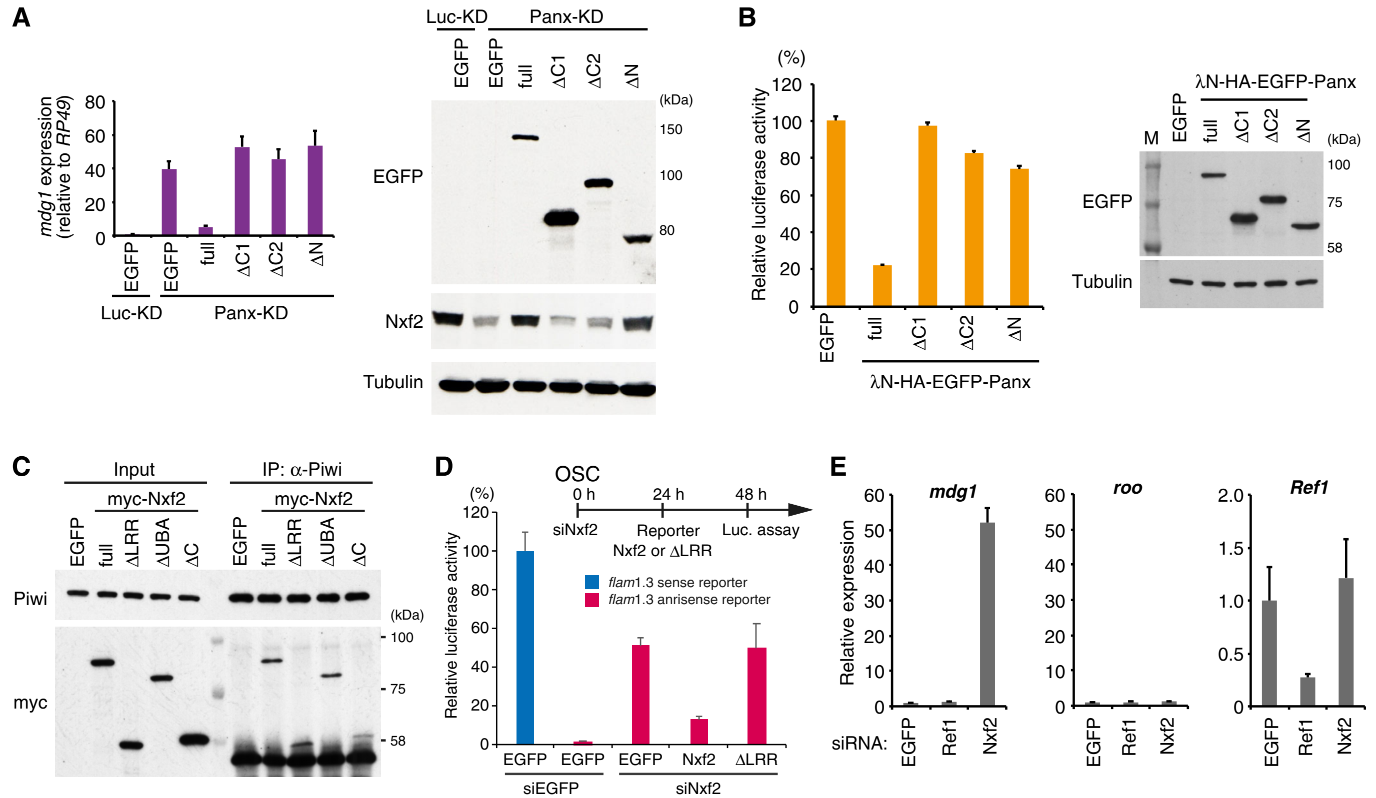

Figure EV5. Both N-terminal and C-terminal regions of Panx are essential for TE silencing.

A EGFP-tagged Panx deletion constructs were expressed in Luc- (control) or Panx-depleted OSCs. *mdg1* expression levels were monitored by qRT–PCR. Expression values are normalized by the expression of *RP49*. Error bars indicate SD (n = 3) (left panel). Western blotting (WB) with an antibody against EGFP, Nxf2, and Tubulin using lysates from transfected OSCs (right panel). The deletion mutants that cannot interact with Nxf2 or Panx could not induce silencing of TE. In addition, the C-terminal region of Panx (400–541 aa) is required for silencing of TE and stable expression of Nxf2.

B Luciferase fluorescence level in OSCs expressing boxB reporter luciferase and the indicated λN fusions (Panx deletion mutants). Error bars indicate SD (n = 4) (left panel). WB of lysates from OSCs expressing boxB reporter luciferase and the indicated λN fusions using EGFP and tubulin antibody (right panel). The deletion mutants that cannot interact with Nxf2 or Panx could not induce silencing upon recruitment to reporter RNA.

C Immunoprecipitation (IP) from lysate of OSCs expressing myc-tagged Nxf2 proteins using anti-Piwi antibody, followed by WB using anti-myc and -Piwi antibodies. All mutant proteins of Nxf2 can interact with Piwi in OSCs.

D Silencing of reporter gene harboring *flam* element (1.3 kbp, antisense) occurs in an Nxf2-dependent manner. Transfection schedule of siRNA and plasmids is shown at the top of the figure. Exogenous expression of Nxf2 protein repressed reporter gene activity in OSCs, but that of Nxf2-ΔLRR protein did not. Error bar indicates SD (n = 3).

E RNA levels of *mdg1*, *roo*, and *Ref1* were quantified by qRT–PCR upon depletion of EGFP (control), Ref1, or Nxf2. Expression levels are normalized by the expression of *RP49*. Error bars represent SD (n = 3). Although Ref1 knockdown significantly decreased the expression level of *Ref1*, *mdg1* TE was unaffected.

© 2019 The Authors

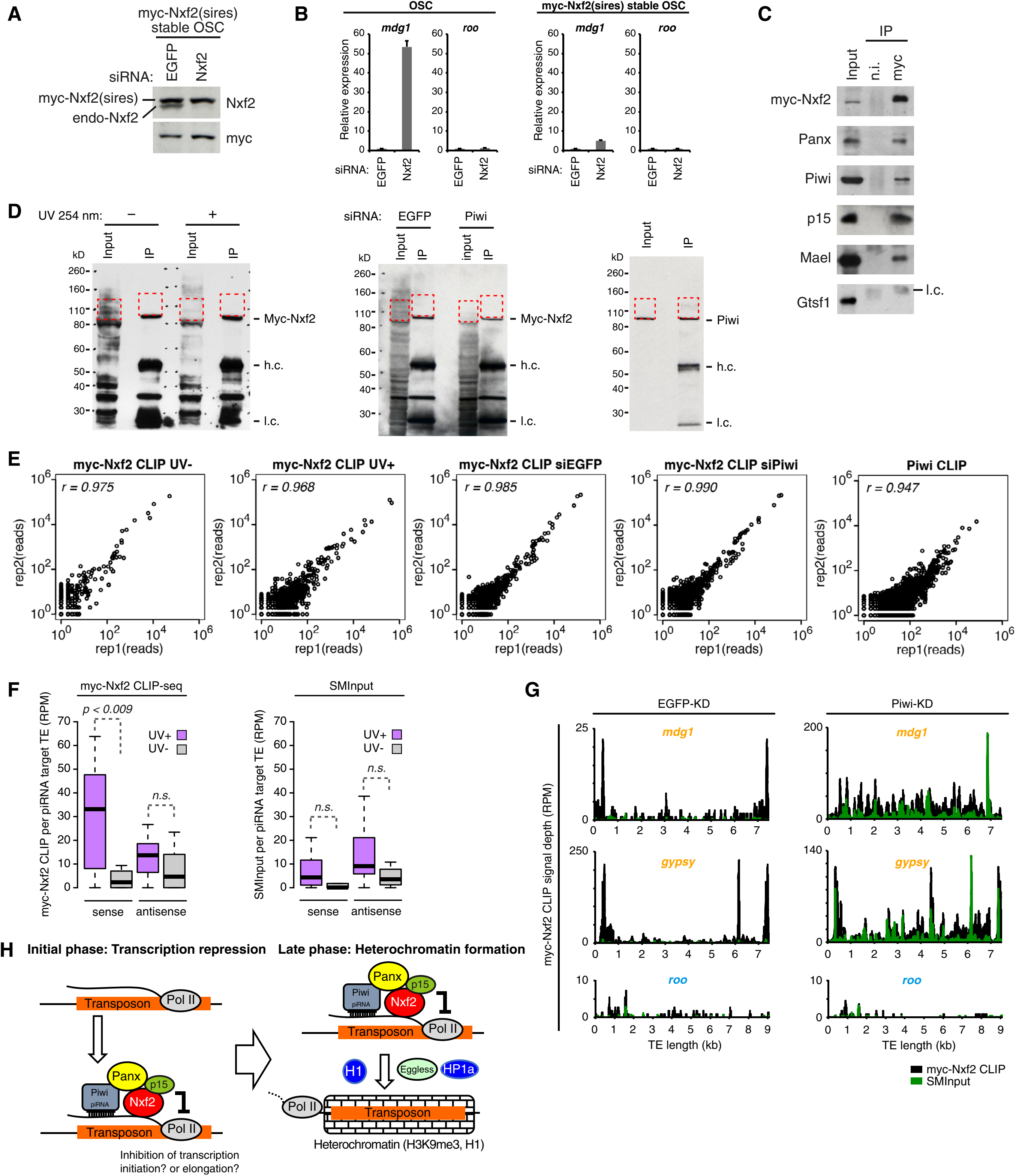

Figure EV6.

Figure EV6. Stably expressed myc-Nxf2 associates with transcripts of Piwi-piRNA target TEs.

A Western blotting (WB) of myc-Nxf2 stable OSC lysate, using Nxf2 and myc antibody upon knockdown of EGFP (control) or Nxf2. Note that expressed myc-Nxf2 is resistant to siRNA.

B RNA levels of *mdg1* and *roo* were quantified by qRT–PCR upon depletion of EGFP (control) or Nxf2. Expression levels are normalized by the expression of *RP49*. Error bars represent SD (n = 3). In OSCs without myc-Nxf2 expression, *mdg1* is de-silenced upon Nxf2-KD, whereas in the myc-Nxf2-expressing stable line, *mdg1* remains silenced.

C Immunoprecipitation (IP) from myc-Nxf2-expressing OSC lysate using anti-myc antibody, followed by WB of myc-Nxf2 (by myc antibody), Panx, Piwi, p15, Mael, and Gtsf1. l.c.: light chain from the antibody.

D WB of myc-Nxf2 IP during CLIP from non-irradiated or UV-irradiated cells (left panel). WB of myc-Nxf2 IP during CLIP from EGFP or Piwi knockdown cells (middle panel). WB of Piwi IP during CLIP (right panel). Red dotted line indicates the region excised for CLIP library preparation.

E Scatter plots of obtained CLIP reads in two biological replicates of indicated CLIP experiments. Each dot represents the read count of the peak called using the Piranha peak-calling algorithm (Uren *et al*, 2012).

F Boxplots showing piRNA-targeted TE-mapped read counts (RPM) obtained from myc-Nxf2 CLIP or SMInput, based on CLIP-seq performed on UV-irradiated and non-irradiated OSCs. Reads mapped in sense and antisense directions were calculated separately. Boxplot central bands, boxes, and whiskers show median, third quartile, first quartile, maxima, and minima, respectively. P-values were calculated by Wilcoxon rank-sum test.

G Density plots for myc-Nxf2 CLIP signal depth over the consensus sequence from *mdg1*, *gypsy* (targeted by Piwi–piRNA, in orange letters), and *roo* (not targeted by Piwi–piRNA, in blue letters) TEs in EGFP-, Piwi-KD OSCs. Reads obtained in myc-Nxf2 CLIP samples are indicated in black, where SMInput is indicated in green.

H Schematic model showing the two-phase regulation of TEs by Piwi–piRISC. Nxf2 forms a complex with Panx, Piwi, and p15 and associates with nascent RNA of target transposable elements. This complex regulates transcription of the TE by the inhibition of Pol II (initial phase). The co-transcriptionally regulated TE shifts to heterochromatin formation, mediated by H3K9me3 marks and H1 (late phase).

© 2019 The Authors